

Fingerprint-Based Visible Light Positioning using Multiple Photodiode Receiver

Adli Hasan, Tyrel Glass, Fakhrol Alam, *and* Mathew Legg

Department of Mechanical & Electrical Engineering, SF&AT, Massey University, New Zealand

Email: adlihasanhasanadli@gmail.com, {t.glass, f.alam, m.legg}@massey.ac.nz

Abstract—Visible Light Positioning (VLP) is a promising indoor localization method as it provides high positioning accuracy and allows for leveraging the existing lighting infrastructure. Photodiode (PD)- based receiver is a commonly used tag for VLP. However a tag employing single PD requires three or more luminaires to be visible. This paper presents a VLP system that uses a custom made tag utilizing multiple PDs. It applies Received Signal Strength (RSS)-based fingerprinting using Weighted k-Nearest Neighbor (WkNN) algorithm for localization. Experimental results show that it is possible to localize using less than three luminaires with high accuracy. Manhattan and Matusita distance metrics are found to provide lower localization accuracy than the Euclidean metric for the WkNN algorithm.

Index Terms—Indoor localization, indoor positioning system (IPS), visible light positioning (VLP), weighted k-nearest neighbors (WkNN)

I. INTRODUCTION

The Global Positioning System (GPS) has been used in many applications such as localization, navigation, tracking, mapping and timing. Although GPS can be used to locate a target outdoors, it is very difficult to do so if the target is located indoors due to its low accuracy resulting from the inability of GPS signals to penetrate through walls [1].

The ability to accurately determine the position of a person or an object indoors can be used in many applications like navigation in large indoor environments such as airports or shopping malls [2].

There are multiple technologies which can be used for indoor localization such as wireless [3], visible light [4] and ultrasound [5]. Wireless-based technologies are vulnerable to multipath and interference [6] whilst ultrasound comes with high installation costs [7].

Recently, visible light-based positioning systems have garnered the interest of researchers due to the convenience of implementation using Light Emitting Diode (LED) luminaires. Visible light signals do not pass through walls making them secure [8] and visible light-based positioning systems can potentially offer higher accuracy compared to other technologies [9].

The most popular type of Visible Light Positioning (VLP) technique is using the Received Signal Strength (RSS) [10]. RSS values obtained from a single Photodiode (PD) can be used to determine the distance between the transmitter (i.e. the luminaire) and receiver/tag [11]. Based on this, techniques such as trilateration [12] and fingerprinting [13] can be applied for localization. A single PD-based VLP system requires at least

three LED luminaires for effective localization. A problem with this is that three or more luminaires may not be visible to the PD in some real-world environments. To overcome this problem, multiple PD VLP systems that can function with less than three luminaires within the PD's Field of View (FOV) have been proposed [14-17].

II. RELATED WORK

Visible light characteristics that are commonly used for VLP are RSS, time of arrival (TOA) [18], time difference of arrival (TDoA) [19] and angle of arrival (AoA) [20].

RSS-based systems can have low accuracy due to sensitivity and tilt issues [21] while AoA-based systems have a higher accuracy compared to RSS but is more complex [22]. TDoA-based systems can achieve high localization accuracy [19] but are more complex and costly to implement as they require synchronization between hardware [23].

RSS-based systems are easy to implement and is less complex with the only downside being accuracy. Multiple PD receivers have been proposed to mitigate the tilt issue [24] with single PD receivers in VLP systems and to enable the system to operate with lower number of luminaires.

A. Multiple Photodiode Systems

Several multiple VLP systems using three [14, 16, 17, 19, 25] or more [4, 9, 26, 27] PDs have been proposed. The systems show that less than three luminaires can be used for localization if multiple PDs are used.

The difference in angles and position of a multi PD receiver design can be exploited to develop new localization methods. For example, using RSS from multiple photodiodes, the RSS Ratio [17, 26, 27] and RSS Difference [16] between the photodiodes can be used to estimate the position of the receiver. Authors from [4] used the linear independence of the multiple photodiode planes while authors from [9] utilized the RSS and incidence angle. It should be noted that, single PD systems that uses a rotating receiver [15, 28, 29] can also emulate multiple PD-based systems. Researchers have proposed a VLP system using a rotatable single-PD receiver where the receiver takes the RSS at a single location at different angles [24]. The authors further developed this system by using the same positioning method but using a receiver with three tilted photodiodes instead [25].

B. Fingerprinting

Fingerprinting method includes two phases: offline and online [30]. In the offline phase, fingerprints or features of an environment are collected in the form of RSS, AoA or TDoA at

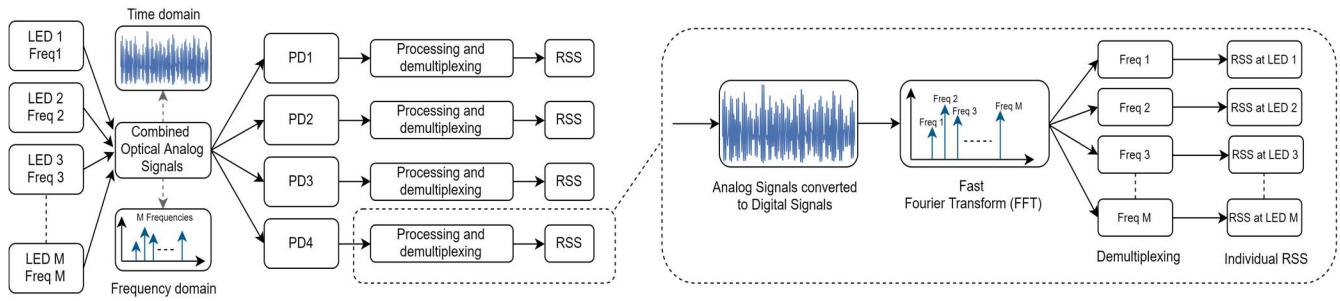


Fig. 1. Block diagram showing how optical signals from the luminaires are processed

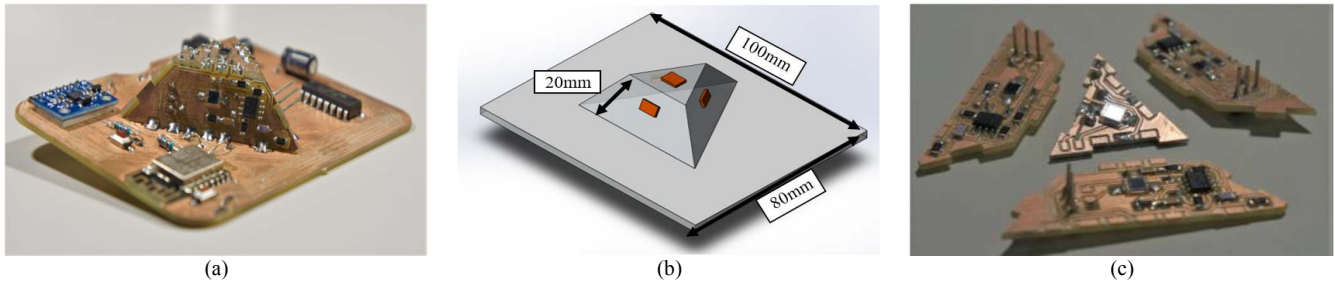


Fig. 2. Custom-made receiver board with three tilted photodiodes and one horizontal photodiode. (a): actual board; (b): 3D Model of the custom-made receiver board with three tilted photodiodes and one horizontal photodiode (marked orange); (c): individual pieces of the receiver before assembling

the target device and is stored in a database. In the online phase, the data obtained from the target in real-time is then compared to the values stored in the database and the position of the device is estimated.

All implementation of reported multiple PD-based VLP systems utilize RSS-distance channel modelling and there is a lack of literature in fingerprint-based multiple PD systems. Therefore in this work, we are exploring a multiple PD fingerprint-based system that can potentially facilitate the application of machine learning techniques for localization.

III. SYSTEM OVERVIEW

The developed VLP system is based on Frequency-Division Multiplexing (FDM) with the demultiplexing done at the receiver through Fast Fourier Transform (FFT). Figure 1 shows a block diagram of the process where M luminaires transmit M discrete tones. At the multiple PD receiver board, the FFT of the optical signals is computed and the received power at the unique frequencies are used as a measure of RSS for the corresponding luminaire.

A. Transmitter

Custom modulation boards were used to drive four consumer grade LED luminaires so that each luminaire is able to transmit unmodulated sine waves at frequencies between 2 kHz-4 kHz [31]. The luminaires are set to transmit unique frequencies of 2.5 KHz, 2.7 KHz, 3.2 KHz and 3.5 KHz respectively to the receiver.

B. Receiver

To receive the optical signals from the luminaires, a custom-made receiver board using an ESP8266 microcontroller was designed. The design of the receiver board is a triangular base with three PDs tilted at an angle of 60° and a single horizontal PD located in the middle as shown in Fig. 2.

A two-stage op-amp circuit was designed to capture the discrete tone signals from the luminaires through the reverse bias current of a PD. The current is then converted into a voltage signal and is read by an ADC which has a sampling rate of 20 kHz. The op-amp circuit is also able to filter out low frequency (e.g. 100 Hz powerline flicker) and steady state DC signals generated by ambient light. The lower corner frequency and upper corner frequency of the op amp is designed to be 550 Hz and 4800 Hz respectively. The receiver board also includes an accelerometer to measure the orientation of the receiver if needed.

C. Data Collection and Experimental Setup

The vertical distance between the receiver board and the luminaires is 1600 mm. A 2D CNC machine with dimensions of 1200 mm x 1200 mm was utilized for taking measurements. The position of the CNC machine can be controlled by providing the XY coordinate of the desired location. The CNC machine has an accuracy of 0.025 mm making it useful for recording the ground truth. The custom-made receiver board was mounted onto the CNC machine to ensure that its orientation is kept constant throughout the experiment. Figure 3 shows the experimental setup with the luminaires, CNC machine and receiver board.

IV. WEIGHTED K-NEAREST NEIGHBORS (WKNN)

Once the offline database has been constructed, the WkNN algorithm can be implemented as a regressor to estimate the position of the receiver during the online stage.

The WkNN algorithm is similar to the k -Nearest Neighbor (kNN) algorithm such that computes the distances of the neighbors. Additionally, the WkNN algorithm also computes the weights of the distances such that the neighbor with the smaller distance will have a greater weighting compared to the neighbor with a greater distance. Let the offline location be

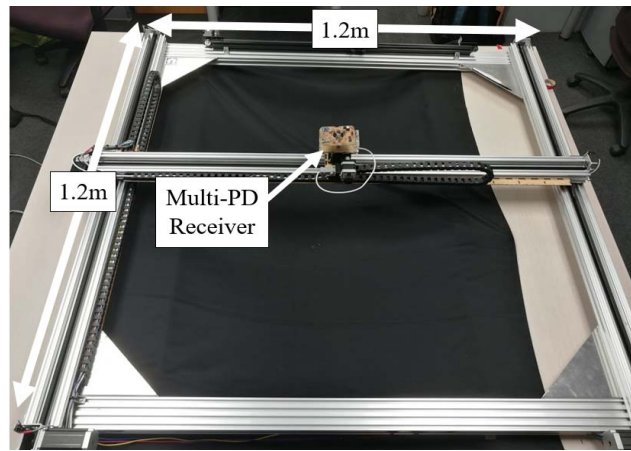
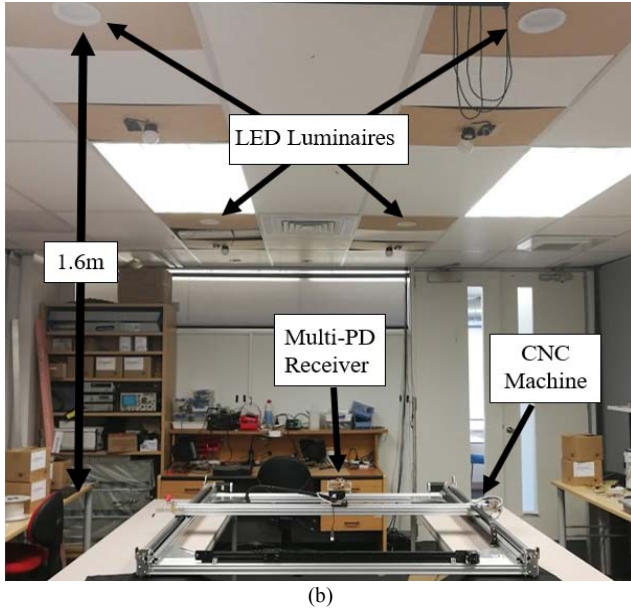
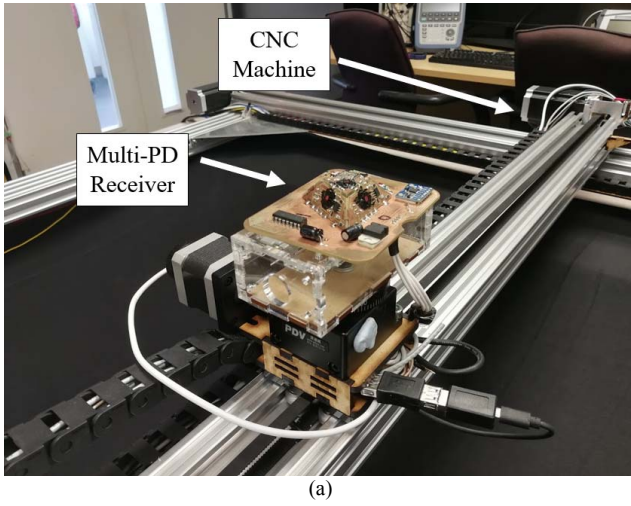


Fig. 3. Experimental setup. (a): Multiple PD receiver mounted onto the CNC machine; (b): VLP Fingerprinting testbed; (c): Top view of CNC machine and multiple PD receiver.

denoted as (x_i, y_i) while the online location is denoted as (x_j^{live}, y_j^{live}) .

The distance $d_{i,j}$ between (x_i, y_i) and (x_j^{live}, y_j^{live}) is computed using a distance metric with the *Euclidean* distance

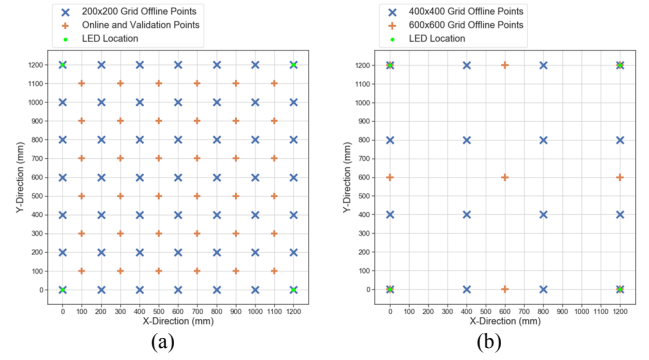


Fig. 4. Location of LED luminaires and measurement locations. (a): location of points used for online validation, offline 200x200; (b): Offline measurement locations for 400x400 and 600x600 grid

TABLE I
LOCALIZATION ERROR FOR VARYING GRID SIZE

Database	Localization error (mm)			
	Median	Std	Max	90 th Perc.
200 mm x 200 mm	3.78	3.02	13.76	8.32
400 mm x 400 mm	25.48	35.33	176.32	93.06
600 mm x 600 mm	82.21	42.24	150.78	128.71

being the most common. The k -Nearest Neighbors are chosen such that they have the smallest distance and the largest weighting. The estimated position of the receiver, $(\tilde{x}_j, \tilde{y}_j)$ is computed as the weighted average of the location of the k -Nearest Neighbors and is given by

$$\tilde{x}_j = \frac{\sum_{b=1}^k w_{j,b} \times x_b}{\sum_{b=1}^k w_{j,b}}, \quad \tilde{y}_j = \frac{\sum_{b=1}^k w_{j,b} \times y_b}{\sum_{b=1}^k w_{j,b}}$$

where (x_b, y_b) is the location of the b -th neighbor from the k -Nearest Neighbors [32]. The value of k needs to be chosen carefully. If a small k is used, it will not fit the data well while a large k will lead to overfitting [33].

V. EXPERIMENTAL RESULTS

169 equally spaced measurements were taken at 100 mm-intervals within the 1200 mm x 1200 mm space. Some of the points are used to construct an offline database corresponding to a 200 mm x 200 mm grid while the rest are used for the online phase and validation as shown in Fig. 4(a). At each location, the RSS at each photodiode for each luminaire was recorded. Since the system uses four luminaires and four PDs, a total of 16 readings were taken at one location.

A. Effects of grid size

Figure 4(b) shows the offline locations for the 400 mm x 400 mm and 600 mm x 600 mm grid. Figure 5 shows that $k=4$ is the most optimum for the 200 x 200 grid while $k=3$ for the 400 x 400 and 600 x 600 grid using four PDs and four luminaires. Table I shows the trade-off between the grid size and the localization error such that increasing the grid size increases the localization error. The accuracy of a fingerprint-based system

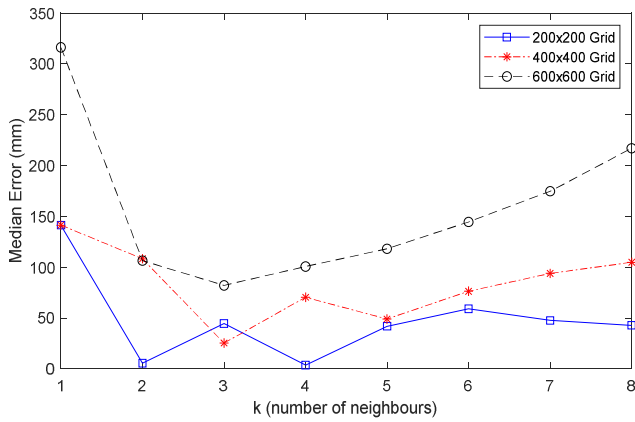


Fig. 5. Median error across varying k values for various grid size using four PDs and four luminaires

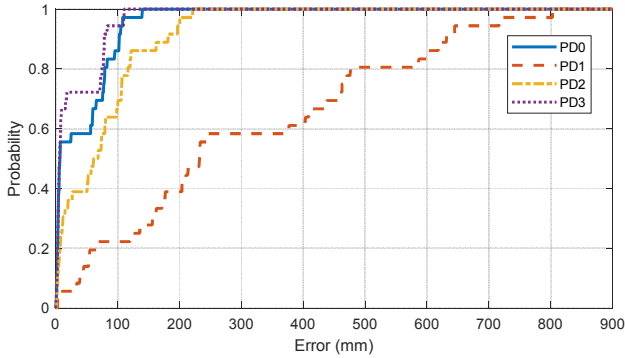


Fig. 6. Localization error for various photodiodes on the receiver board using the 200x200 grid, $k=4$ and four luminaires

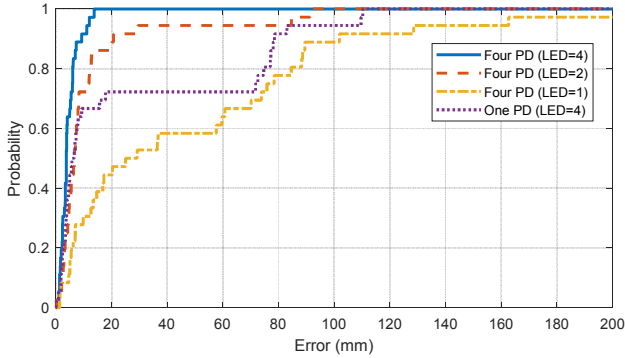


Fig. 7. Localization error for different combination of PDs and LEDs

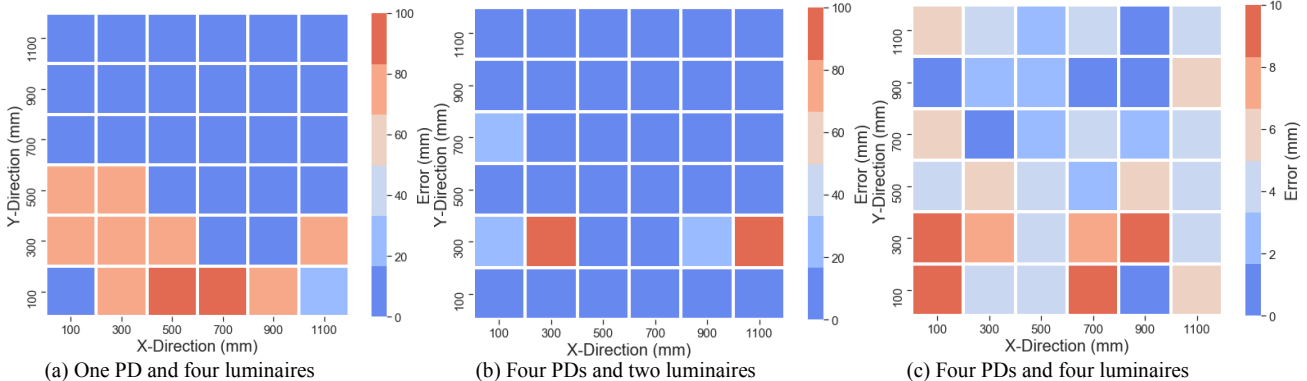


Fig. 8. Localization error based on the X and Y locations of the online points for various luminaire and PD combinations

is determined by the size of the offline database. A larger database requires more time in offline site survey but provides higher localization accuracy.

B. Single photodiode selection

The receiver has a total of four individual PDs. Figure 6 presents the Cumulative Distribution Function (CDF) of the localization error for the 200x200 grid ($k=4$ and four luminaires). It can be observed that PD3 outperforms the rest of the PDs. It is important to note that it is the horizontal PD. Therefore it has all four luminaires in its FOV throughout the experiments and has the smallest localization error. This allows it to be used to emulate a single-PD system for comparison purposes. Based on the orientation of the receiver, PD1 has only two luminaires within its FOV throughout the whole experiment. As for PD0 and PD2, it was found that they have three luminaires within their FOV for at least half the measurement locations. Moving forward, experiments using “one photodiode” would refer to the ones using RSS from the horizontal PD, PD3.

C. Effects of number of PDs and luminaires

Table II shows the trade-off between number of luminaires used and the localization accuracy. Increasing the number of luminaires increases the localization accuracy. However, with the four PD-based system, a median error of 6.63 mm and 90th percentile error of 20.45 mm can still be achieved using only two luminaires. For the four PD system, the localization accuracy degrades significantly only for the one luminaire scenario. The other observation is that a higher localization accuracy can be achieved using four PDs compared to using a single PD for the same number of luminaires. It is also obvious from the results that the performance of the single PD-based system degrades significantly when the number of luminaires is less than 3.

Figure 7 shows the CDF of the localization error for different combinations of PDs and luminaires. It shows that the four PD and two LED system outperforms the one PD and four LED system. The heatmap in Fig. 8 shows the errors of the online points with reference to their X and Y locations (in mm) for different PD and luminaire combinations. The heatmaps show that most of the large errors are located at the lower half of the grid. The errors in the lower part of the grid for the one PD and four luminaires system can be reduced by using four PD and two luminaires as shown in Fig. 8 (a) and (b). By using four

TABLE II
LOCALIZATION ERROR FOR ONE AND FOUR PHOTODIODES USING DIFFERENT NUMBER OF LEDs FOR 200x200 GRID ($K=4$)

Number of LED	Localization Error (mm)							
	One Photodiode				Four Photodiodes			
	Median	Std	Max	90 th Percentile	Median	Std	Max	90 th Percentile
1	348.33	280.28	1116.10	775.71	27.10	48.03	200.26	95.67
2	96.89	119.46	410.45	334.89	6.63	19.29	91.30	20.45
3	60.95	32.99	87.54	78.97	5.37	10.58	65.25	11.24
4	6.17	35.83	110.26	78.31	3.78	3.02	13.76	8.32

TABLE III
LOCALIZATION ERROR FOR VARIOUS DISTANCE METRIC USING FOUR PD AND FOUR LUMINAIRES ($K=4$).

Distance Metric	Localization Error (mm)			
	200 x 200		400x400	
	Median	90 Perc.	Median	90 Perc.
Euclidean	3.78	8.33	25.48	93.07
Manhattan	3.15	5.48	22.1	37.05
Chebyshev	10.57	18.36	40.24	122.54
Squared Euclidean	7.53	15.81	62.4	77.33
Squared Chord	6.47	14.46	61.76	78.58
Matusita	3.42	7.53	24.25	31.47
Canberra	3.89	6.65	26.16	118.2
Lorentzian	1.15	3.4	41.37	155.06

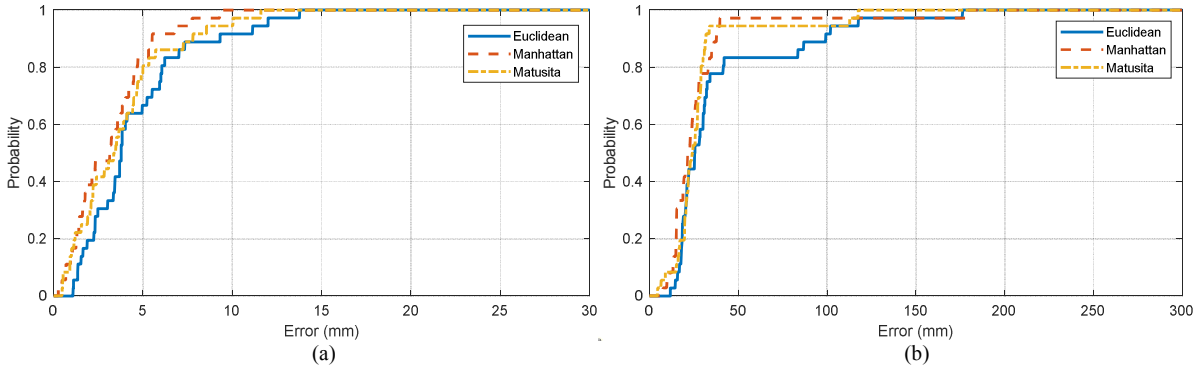


Fig. 9. Localization error of Euclidean, Manhattan and Matusita distance metric using four PDs and four luminaires for different scenarios. (a): Localization error for 200 mm x 200 mm; (b): Localization error for 400 mm x 400 mm

PDs and four luminaires, the errors can be significantly reduced by an order of magnitude as shown in Fig. 8 (c). It also shows that the larger localization errors are still located at the lower part of the grid indicating that the errors may be resulting from multipath and reflection. The orientation of the receiver might not be the most optimal orientation where the luminaires are not within the FOV of the PDs. Noise from the hardware and resolution of the ADC can also contribute to the error.

D. Impact of distance metrics

As discussed in Section IV, the distance $d_{i,j}$ between (x_i, y_i) and (x_j^{live}, y_j^{live}) is computed and the weight of the WkNN regressor is then estimated as the reciprocal of the distance. While Euclidean distance metric is most commonly used, literature [32] shows that the localization accuracy of a VLP using WkNN depends on the distance metrics utilized. Consequently, eight different distance metrics were explored and used to compute the weights for the WkNN algorithm. Table III shows the localization error for the various distance

metrics using four PDs and four luminaires. It can be observed that the Euclidean distance is one of the better performing metrics. However, Manhattan and Matusita distance outperform the Euclidean distance for all scenarios. These three distance metrics were benchmarked in Fig. 9 by plotting the CDF of localization error.

VI. CONCLUSION

This paper presents a visible light-based positioning method using four photodiodes. Within a testbed of 1.2 m x 1.2 m, median error of 3.78 mm can be achieved for four luminaires while a median error of 6.63 mm can be achieved with two luminaires. The multiple PD-based system have higher localization accuracy and can function with less number of visible luminaires compared to a single PD-based system. The localization error can be further reduced by selecting either the Manhattan or the Matusita distance metrics for the WkNN algorithm.

Throughout the experiments, the orientation of the receiver was kept unchanged. While this is a realistic assumption for robotic applications (a simple gimbal can achieve this), the impact of orientation change needs to be explored. In a real-world environment, online points would not always be on a regular grid hence spontaneous online points can be used to test the performance in such a scenario. Future work could also include implementing model-based localization using the multi-PD receiver board. A comparative benchmarking against existing solutions has also been left for future investigation.

Acknowledgment

The authors acknowledge Baden Parr who contributed to the development of the hardware.

REFERENCES

1. Enge, F.v.d.a.P. *The World's first GPS MOOC and Worldwide Laboratory using Smartphones*. in *Proceedings of the 28th International Technical Meeting of the Satellite Division of The Institute of Navigation (ION GNSS+ 2015)*. 2015. Tampa, Florida,.
2. *Indoor Navigation & Services in Airports*. [cited 2019 10 October]; Available from: <https://www.infsoft.com/industries/airports/features>.
3. Bianchi, V., P. Ciampolini, and I.D. Munari, *RSSI-Based Indoor Localization and Identification for ZigBee Wireless Sensor Networks in Smart Homes*. IEEE Transactions on Instrumentation and Measurement, 2019. **68**(2): p. 566-575.
4. Xie, B., et al., *LIPS: A Light Intensity--Based Positioning System for Indoor Environments*. ACM Trans. Sen. Netw., 2016. **12**(4): p. 1-27.
5. Carotenuto, R., et al., *An Indoor Ultrasonic System for Autonomous 3-D Positioning*. IEEE Transactions on Instrumentation and Measurement, 2019. **68**(7): p. 2507-2518.
6. Fang, J., et al., *High-Speed Indoor Navigation System based on Visible Light and Mobile Phone*. IEEE Photonics Journal, 2017. **9**(2): p. 1-11.
7. Rabadan, J., et al., *Hybrid Visible Light and Ultrasound-Based Sensor for Distance Estimation*. Sensors (Basel, Switzerland), 2017. **17**(2): p. 330.
8. CHENG, L., et al., *Comparison of Radio Frequency and Visible Light Propagation Channels for Vehicular Communications*. IEEE Access, Access, IEEE, 2018: p. 2634.
9. Yasir, M., S.-W. Ho, and B.N. Vellambi, *Indoor Position Tracking Using Multiple Optical Receivers*. Journal of Lightwave Technology, Lightwave Technology, Journal of, J. Lightwave Technol., 2016(4): p. 1166.
10. Yang, Z., et al., *Wearables Can Afford: Light-weight Indoor Positioning with Visible Light*, in *Proceedings of the 13th Annual International Conference on Mobile Systems, Applications, and Services*. 2015, ACM: Florence, Italy. p. 317-330.
11. Zhuang, Y., et al., *A Survey of Positioning Systems Using Visible LED Lights*. IEEE Communications Surveys & Tutorials, 2018. **20**(3): p. 1963-1988.
12. See, Y.C., N.M. Noor, and Y.M. Calvin Tan. *Investigation of Indoor Positioning System using Visible Light Communication*. in *2016 IEEE Region 10 Conference (TENCON)*. 2016.
13. Liu, W., et al. *Smallest enclosing circle-based fingerprint clustering and modified-WKNN matching algorithm for indoor positioning*. in *2016 International Conference on Indoor Positioning and Indoor Navigation (IPIN)*. 2016.
14. Yang, S., E. Jung, and S. Han, *Indoor Location Estimation Based on LED Visible Light Communication Using Multiple Optical Receivers*. IEEE Communications Letters, 2013. **17**(9): p. 1834-1837.
15. Yang, S. and S. Han. *VLC based indoor positioning using single-Tx and rotatable single-Rx*. in *2014 12th International Conference on Optical Internet 2014 (COIN)*. 2014.
16. Xu, W., et al., *Indoor Positioning for Multiphotodiode Device Using Visible-Light Communications*. IEEE Photonics Journal, 2016. **8**(1): p. 1-11.
17. Yu, X., J. Wang, and H. Lu, *Single LED-Based Indoor Positioning System Using Multiple Photodetectors*. IEEE Photonics Journal, 2018. **10**(6): p. 1-8.
18. Akiyama, T., M. Sugimoto, and H. Hashizume. *Time-of-arrival-based smartphone localization using visible light communication*. in *2017 International Conference on Indoor Positioning and Indoor Navigation (IPIN)*. 2017.
19. Naz, A., et al. *Single LED ceiling lamp based indoor positioning system*. in *2018 IEEE 4th World Forum on Internet of Things (WF-IoT)*. 2018.
20. Arafa, A., X. Jin, and R. Klukas, *Wireless indoor optical positioning with a differential photosensor*. IEEE Photonics Technology Letters, 2012. **24**(12): p. 1027-1029.
21. Zhang, S., et al., *Experimental Demonstration of Indoor Sub-Decimeter Accuracy VLP System Using Differential PDOA*. IEEE Photonics Technology Letters, 2018. **30**(19): p. 1703-1706.
22. Steendam, H., T.Q. Wang, and J. Armstrong. *Cramer-Rao bound for AOA-based VLP with an aperture-based receiver*. in *2017 IEEE International Conference on Communications (ICC)*. 2017.
23. Nah, J.H.Y., R. Parthiban, and M.H. Jaward. *Visible Light Communications localization using TDOA-based coherent heterodyne detection*. in *2013 IEEE 4th International Conference on Photonics (ICP)*. 2013.
24. Jeong, E., et al., *Tilted receiver angle error compensated indoor positioning system based on visible light communication*. Electronics Letters, 2013. **49**(14): p. 890-892.
25. Yang, S.-H., et al., *Three-Dimensional Visible Light Indoor Localization Using AOA and RSS With Multiple Optical Receivers*. 2014. p. 2480-2485.
26. Yu, X., J. Wang, and H. Lu. *Indoor Positioning System Based on Single LED Using Symmetrical Optical Receiver*. in *2018 Asia Communications and Photonics Conference (ACP)*. 2018.
27. Wang, L. and C. Guo. *Indoor Visible Light Localization Algorithm with Multi-Directional PD Array*. in *2017 IEEE Globecom Workshops (GC Wkshps)*. 2017.
28. Yasir, M., S. Ho, and B.N. Vellambi, *Indoor Positioning System Using Visible Light and Accelerometer*. Journal of Lightwave Technology, 2014. **32**(19): p. 3306-3316.
29. Xie, B., S. Gong, and G. Tan, *LiPro: light-based indoor positioning with rotating handheld devices*. Wireless Networks (10220038), 2018. **24**(1): p. 49-59.
30. Alraih, S., et al. *Improving accuracy in indoor localization system using fingerprinting technique*. in *2017 International Conference on Information and Communication Technology Convergence (ICTC)*. 2017.
31. Alam, F., B. Parr, and S. Mander, *Visible Light Positioning Based on Calibrated Propagation Model*. IEEE Sensors Letters, 2019. **3**(2): p. 1-4.
32. Alam, F., et al., *An Accurate Visible Light Positioning System Using Regenerated Fingerprint Database Based on Calibrated Propagation Model*. IEEE Transactions on Instrumentation and Measurement, 2019. **68**(8): p. 2714-2723.
33. Gou, J., et al., *A New Distance-weighted k -nearest Neighbor Classifier*. J. Inf. Comput. Sci., 2011. **9**.